POSTER SESSIONS I-IV

THE FIBROSIS AND OTHER MORPHOLOGIC CHANGES OF RAT LUNG CAUSED BY INTRATRACHEAL INJECTION OF DIFFERENT SIZES OF METALLIC ALUMINUM DUSTS

ZHOU CHEN, M.D. • Chen Hongchuang, M.D.

Department of Public Health, China Medical University, Shenyang, People's Republic of China

INTRODUCTION

The study of relationship between pulmonary biological effect and sizes of dust is the basis for toxicological evaluation of dust and setting up dust sampling curve.[1,2] Although there were a few of this kind of studies in the past, it has not been intensively investigated. Several studies concerning the fibrogenic effect of different sizes of silica dust showed that the strongest fibrogenic size is under 5 μm, and particle size influenced the fibrotic response and other morphological characteristics of animal lung.[3,4,5] There was no study of the fibrogenic effect of different sizes of dust other than silica, such as metal dust. Also the morphological characteristics of animal lung caused by different sizes of dusts has not been evaluated thoroughly. In this paper, we present the experimental result of our studies of biological effects of different sizes of metallic aluminum dusts.

MATERIALS AND METHODS

Aluminum Dusts

Metallic aluminum dusts were obtained from an aluminum company which manufactured aluminum powders with different sizes. The powders were repeatedly separated by the method of sedimentation in ethyl ether. The particles with 1 μm, 5 μm, 10 μm, 15 μm optic diameters were collected, then these particulates were further separated by particulate centrifuge. The optic diameters of the separated aluminum particles were determined under microscope and presented in Table I. The chemical composition of these aluminum particulates were: aluminum, 96%; alumina, 3%; ferric oxides, 0.3%. No toxic heavy metals were detected (atomic absorption spectrometry).

Animal

Wistar outbred strain male rats weighing between 200 and 250 g were used for experiment.

Intratracheal Injection

50 mg of aluminum dust was suspended in 1.0 ml of saline. 5 groups of rats were used. Each group of rats were intratracheally injected respectively with 1.0 ml of 1 μm, 5 μm, 10 μm, 15 μm aluminum dust suspension or saline. The rats were sacrificed 6, 9 months after injection. A total of 100 rats were evaluated in this study and about 10 rats were evaluated in each group at each time point.

Lung Weight and Collagen Content

5 rats in each group were sacrificed with overdose of pentobarbital and their thoracic cavity was opened immediately. After removal of heart and tracheal, the wet lung weight was recorded. The dry weight of the lung was determined after the lung was cut into small pieces and dried in 110°C for 2 hours. The hydroxyproline was analyzed by acid hydrolysis of these dry pieces of lung tissue. The collagen content was estimated from determination of hydroxyproline.

Morphological Studies

About 5 rats in each group were sacrificed and their lungs were instilled drop by drop with 10% formalin. A longitudinal section of the lung, and the lymph node were cut and embedded in paraffin. The sections were stained with hematoxylin and eosin (HE), and also stained for reticulin and collagen.

The histopathologic changes of rat lungs were observed under

Table I

The Particle Sizes of the Experimental Aluminum Dusts

Size (μm)	Size distribution of aluminum particles (%)										
	<1	1-	2.5	2.5-	5	7.5-	10.0	12.5-	15	17.5-	20-
1	5	80	10	4	1						
5			4	10	75	10	1				
10				1	4	8	73	8	3	2	
15						1	2	5	70	18	4

microscope. The degree of nodular fibrosis was evaluated by Belt-King classification. In each lung, left lobe and right lobes were selected to measure the area of nodular fibrosis, area of alveolar wall thickening, area of emphysema. The area of nodular formation and alveolar wall thickening and emphysema were determined under 10 x 10 microscope with a 10 x 10 graticule (3.24 mm^2 in area). 12 locations in each lobe were randomly selected for quantitative observation and 12 lobes were evaluated in each group. The values presented were average of the 144 measurement.

RESULTS

Lung Weight and Collagen Content

Rats injected with aluminum dust had higher lung weight (wet and dry) and total collagen than control rats. The increase of lung weight and collagen content in 5 μm, 1 μm groups had statistical significance when compared with control group. Although the lung weight and collagen content were higher in 10 μm and 15 μm groups than control group, there was no statistical significance. (Figures 1, 2 and Table II)

Among animals exposed to different sizes of dust, the rats injected with 5 μm, 1 μm dusts have significantly higher lung weight and collagen content than those of rats in 10 μm, 15 μm groups. The order of increase of above parameter was: 5 μm > 1 μm > 10 μm > 15 μm. After statistical analysis of difference between each two groups, we found lung wet weight had significant difference between every two groups except the comparison between 10 μm and 15 μm groups. Dry weight and collagen had significant difference between every two groups except no statistical difference between 10 μm and 15 μm groups, 1 μm and 5 μm groups. (Figures 1, 2 and Table II)

Quantitative Lung Morphology

Six and nine months after intratracheal injection with different sizes of aluminum dusts, the major histological changes of rat lung were nodular fibrosis, interstitial fibrosis (or alveolar wall thickening) and emphysema. The degree of nodular fibrosis of rat lung was evaluated by Belt-King's grading. This result was shown in Table III. At end of experiment (9 months after injection), average degree of nodular fibrosis was 3.5 in 5 μm group, 2.6 in 1 μm group, 1.4 in 10 μm and 1.2 in 15 μm groups.

The extent of nodular fibrosis, alveolar wall thickening and extent of emphysema were determined by counting the number of graticules with positive changes in a total of 100 graticule under microscope. Table IV shows these quantitative results. The area (number of graticule with positive histological changes) of nodular fibrosis of rat lung was largest in 5 μm group, smallest in 15 μm group. The 10 μm group had significant larger area of alveolar wall thickening than those of other groups. The areas of emphysema were larger in 10 μm and 15 μm groups than 1 μm and 5 μm groups.

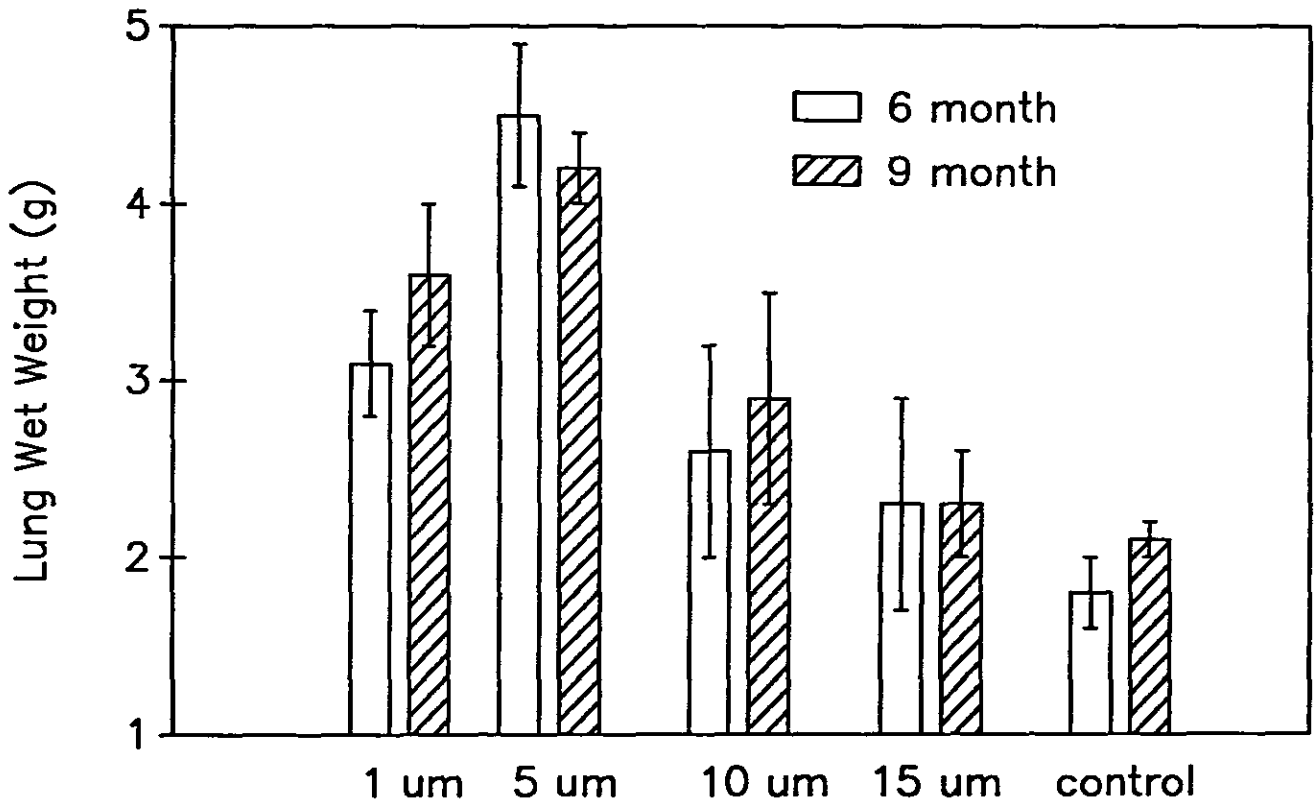

Figure 1. The changes of lung wet weights among rats intratracheally injected with different sizes of aluminum dusts.

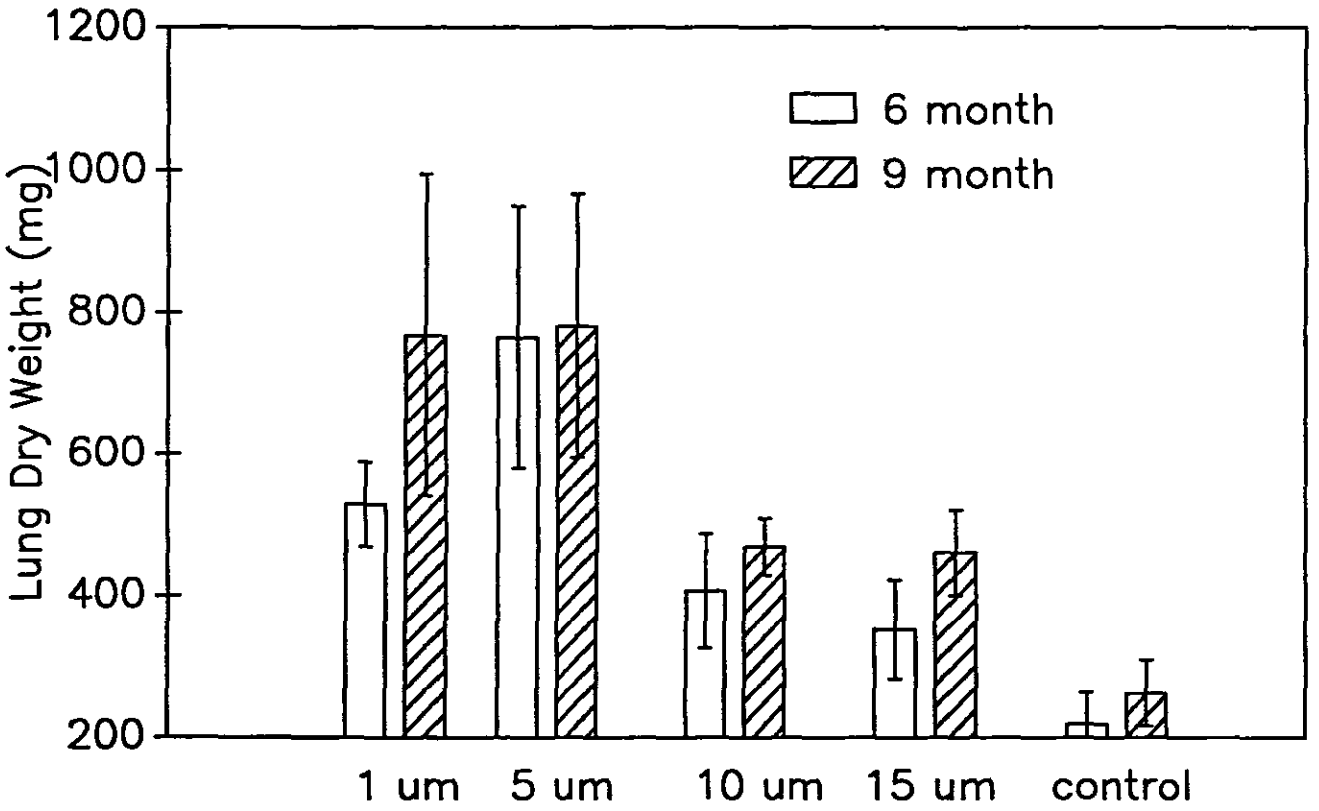

Figure 2. The lung dry weight among rats intratracheally injected with different sizes of aluminum dusts.

Table II

The Lung Collagen of the Rats Administered with Different Sizes of Aluminum Dusts

Group	Time (month)	No.of rats	Collagen (mg) mean	SD
1 μm	6	5	55.0	14.6**
	9	5	65.4	28.4*
5 μm	6	5	74.0	16.2**
	9	4	76.4	16.8**
10 μm	6	5	25.2	7.0
	9	5	34.6	13.2
15 μm	6	5	23.8	4.8
	9	5	23.2	12.1
control	6	5	15.8	3.6
	9	5	22.4	2.6

*: comparing with control group, P<0.05.
**:comparing with control group, P<0.01.

Table III

The Lung Fibrosis of Rats Administered with Different Sizes of Aluminum Dusts

Group	Time (month)	No.of rats	Degree of fibrosis# I	II	III	IV	V	Average
1 μm	6	5	1	2	2	0	0	2.2
	9	5	0	2	3	0	0	2.6
5 μm	6	5	0	2	3	0	0	2.6
	9	4	0	0	2	2	0	3.5
10 μm	6	6	5	1	0	0	0	1.2
	9	5	3	2	0	0	0	1.4
15 μm	6	5	5	0	0	0	0	1.0
	9	5	4	1	0	0	0	1.2

#:Belt-King's grading.

Table IV

The Quantitative Measurement of Areas* of Nodular Fibrosis, Alveolar Wall Thickening, Emphysema

Groups	Time (month)	No.of lung	Area of nodular fibrosis mean	SD	Area of alveolar wall thickening mean	SD	Area of emphysema mean	SD
1 μm	6	12	1.0	0.04	22.7	3.5	4.2	1.7
	9	12	2.8	0.10	15.7	3.3	8.4	1.5
5 μm	6	12	7.2	0.41	24.2	4.1	1.4	0.4
	9	12	6.6	0.22	18.0	4.3	7.2	1.8
10 μm	6	12	2.5	0.21	36.2	3.9	10.1	3.9
	9	12	1.6	0.11	27.3	5.2	17.2	2.9
15 μm	6	12	0.2	0.01	26.5	4.5	8.0	1.9
	9	12	0.3	0.04	17.8	5.6	16.4	3.3
control	6	12	--	--	--	--	2.3	0.7
	9	12	--	--	--	--	2.5	1.2

*: Number of graticule with positive pathologic changes in a total of 10 * 10 graticule (3.24 mm^2) under microscope.

Other Major Morphological Changes

9 months after intratracheal injection, rat lung and lymph nodes in different size groups had their own futures. In rats injected with 1 μm dust,there were slight thickening of alveolar wall with reticulin and slight collagen staining, inflammatory cells infiltration with reticulin and collagen proliferation around bronchiole, dust foci with reticulin staining within lymph nodes. In rats administered with 5 μm aluminum dust, there was significant alveolar wall fibrosis with intensive collagen staining, a large amount of inflammatory cell infiltration and collagen fiber proliferation around bronchiole and many dust-cell foci with collagen staining in lymph nodes. While in the 10 μm group, significant alveolar wall cell proliferation with only mild reticulin increase was observed, there was only slight increase of reticulin around bronchiole and a few dust foci in lymph nodes. The rat lung treated with 15 μm aluminum particles showed only slight alveolar wall thickening or dust deposition and no pathological changes around bronchiole and within lymph nodes. Lung and lymph nodes of control rats were normal.

DISCUSSION

According to the few past experimental studies on silica, the strongest fibrogenic size was below 5 μm. King et al studied 4 kinds of different sizes of silica. He found that the fibrogenicity was strongest in 1–2 μm silica, 0.5–1.0 μm and 2.0–4.0 μm silica were less fibrogenic, 4.0–8.0 μm silica only

produced slight fibrosis.[3] Kysela et al investigated 9 kinds of different silica dusts ranging from 0.7 to 35 μm. He reported that 1 μm silica caused strongest fibrosis response in animal lung, 7–10 μm silica caused cell nodule, 35 μm silica only produced alveolar wall thickening.[4] Goldstein and Webster reported that 2–5 μm silica had stronger fibrosis response than 1–2 μm silica.[5] All these results show that there is a strong fibrogenic size of dust.

In our study, we selected metallic aluminum dust to study the relationship between particle sizes and lung biological response. The metallic aluminum dust was selected because it is a known strong fibrogenic dust.[6,7,8,9] Metallic aluminum dust could cause nodular lung fibrosis, interstitial lung fibrosis and emphysema, which include nearly all chronic pathological changes from inhalation of toxic dust.

After 6, 9 months of intratracheal injection of 50 mg dust, we found 5 μm, 1 μm dusts were more fibrogenic than 10 μm, 15 μm dust. 5 μm and 1 μm aluminum dusts caused grade III even grade IV lung nodular fibrosis, intensive staining of collagen fiber in alveolar wall and higher collagen content than control animals; while 10 μm and 15 μm aluminum dusts produced only grade II or less than grade II lung nodule, increase of reticulin in alveolar wall and no significant increase of lung collagen protein. These results demonstrated that the strong fibrogenic size of metallic aluminum dust was smaller than 5 μm. 10 μm particles were less fibrogenic and 15 μm particles were non fibrogenic. Our results were consistent with those findings in silica.

Between 1 μm and 5 μm aluminum dust, we found 5 μm dust was more fibrogenic. This is similar to Goldstein and Webster's results. The strongest fibrogenic particle of aluminum dust is between 1 μm and 5 μm.

We also found that 10 μm aluminum dust produced significant alveolar wall thickening (cell proliferation) and slight emphysema. Snipes et al reported that 10–13 μm particle was removed from animal lung slower than 7–9 μm particles and even much slower than 3 μm particles.[10–11] Because a considerable amount of particles between 10 μm and 15 μm were found in the lung of pneumoconiosis workers, we should not overlook the biological effect of particles between 10 μm and 15 μm.

We concluded from our study that metallic aluminum particles between 1 μm and 5 μm caused strong fibrosis response and particles larger than 15 μm were not fibrogenic. Although 10 μm particle had slight fibrogenic effect, it produced alveolar wall thickening and slight emphysema. The biological effect of 10 μm particles should not be overlooked.

REFERENCES

1. Xing, G.C.: Advance in Pneumoconiosis Research. *Occup. Med.* 12:43-45 (1985). [in chines]
2. Liu, H.J.: Advance in Dust Control Technology. *Chin. J. Ind. Hyg. Occup. Med.* 3:48-50 (1985). [in chines]
3. King, E.J., Mohanty, G.P., Harrison, C.V., Nagelschmidt, G.: The Action of Flint of Variable Size Injected at Constant Weight and Constant Surface into the Lungs of Rats. *Brit. J. Ind. Med.* 10:76-92 (1953).
4. Kysela, B., Jiraova, D.H., Skoda, V.: The Influence of the Size of Quartz Dust Particles on the Reaction of Lung Tissue. *Ann. Occup. Hyg.* 16:103-129 (1973).
5. Goldstein, B., Webster, I: Intratracheal Injection into Rats of Size-graded Silica Particles. *Brit. J. Ind. Med.* 23:71-74 (1966).
6. Corrin, B.: Aluminum Pneumoconiosis II.Effect on the Rat Lung of Intratracheal Injections of Stamped Aluminum Powders. *Brit. J. Ind. Med.* 20:268-276 (1963).
7. Mitchell, J., Manning, G.B., Molyneux, M., Lane, R.E.: Pulmonary Fibrosis in Workers Exposed to Finely Powdered Aluminum. *Brit. J. Ind. Med.* 18:10-20 (1961).
8. Mclaughlin, A.I.G, Kazantzis, G., King, E., Donald, Teare, Porter, R.J., Owen, R.: Pulmonary Fibrosis and Encephalopathy Associated with the Inhalation of Aluminum Dust. *Brit. J. Ind. Med.* 19:253-263 (1962).
9. Gross, P.: Pulmonary Reaction to Metallic Aluminum Powder. *Arch. Environ. Health* 26:227-236 (1973).
10. Snipes, M.B., Chavez, G.T., Muggenburg, B.A.: Disposition of 3-,7-,and 13-μm Microspheres Instilled into Lungs of Dogs. *Environ. Res.* 33:333-342 (1984).
11. Snipes, M.B., Clem, M.F.: Retention of Microsphere in the Rat Lung after Intratracheal Instillation. *Environ. Res.* 24:33-41 (1981).

RESPIRATORY SYMPTOMS AND LUNG FUNCTION IN JUTE PROCESSING WORKERS: A PRIMARY INVESTIGATION

ZHOU CHEN, M.D. • Zenlin Liu, M.D. • Chinshan Ho, M.D. • Jiezhi Lou, M.D.
Department of Public Health, China Medical University, Shenyang, People's Republic of China

INTRODUCTION

Effect of vegetable dusts on the workers' health has been noticed for many years, but only in recent years has much attention been paid to this occupational problem.[1,2,3] Although there have been a few studies on the health effect of jute dust, little information was available for the chronic effect of jute dust exposure. In the early 1960s, Mair et al and Gilson et al found no "Monday" symptom and no acute lung function injury in jute-dust exposed workers in Britain.[4,5] But a few investigators had reported lung function decrement in the first working shift and atypical chest tightness in jute processing workers in other countries.[6-8] In this report, we conducted an industrial hygiene survey and respiratory symptoms investigation as well as lung function measurements to verify if there was any occupational lung disease problem in the China jute industry. We also attempted to explore the possible mechanisms of the lung injury in this industry.

SUBJECTS AND METHODS

Subjects

404 jute exposed workers were included in the study. The criteria for selecting workers for examination were: (1) at least one year of dust exposure; (2) without asthma, tuberculosis, heart disease; and (3) no current respiratory infection. Among these workers, 217 were male, 187 were female. The control group contained 396 workers coming from the same city and had jobs of similar labor intensity but had not been exposed to toxicant or dust. Among these workers, 236 were male and 160 were female.

Questionnaire

Because the workers rest 24 hours after working for three days, the medical examinations were carried out before the beginning of the first working day. The workers were questioned about their respiratory symptoms by a trained physician. The questionnaire was based on the MRC respiratory symptom questionnaire with emphasis placed on the chronic respiratory symptoms and chronic lung diseases as well as occupational exposure history. Measurement of body weight and height were also conducted.

Lung Functions

Spirometry was performed using a waterseal spirometer. The subject performed the maximum expiratory flow-volume curve and repeated the performance until at least three acceptable curves were obtained. Subjects who did not have acceptable curves were excluded. Lung function analysis was performed on the curve with largest value. Forced vital capacity (FVC), forced expiratory volume in one second ($FEV_{1.0}$), and $FEV_{1.0}$/FVC were measured. Measurements were converted to BTPS. Multiple regression equations were established by use of lung function data from control workers who had no respiratory symptom. When establishing the regression equations, age, height, body weight, smoking and sex were considered as variables. The predicted values of lung function of all workers were calculated according to the established equations. The lower limits of abnormal values were 0.80 for predicted FVC, and 0.75 for predicted $FEV_{1.0}$/FVC. The criteria for selecting abnormal of predicted $FEV_{1.0}$ were selected according to WHO's suggestion: >0.80, normal; 0.79–0.60, slight or moderately abnormal; <0.60, severely abnormal.

Industrial Hygiene Investigation

The jute mill studied consists of two parts: a weaving factory producing jute sacks and a spinning mill producing fine rope. The jute was brought to the mill from various regions in China and then was processed in the following steps: mixing, softening the fiber with mineral water and pressed through a "softener," carding, roving, spinning, winding, weaving, and finishing. The manufacturing procedures in the weaving factory and in the spinning mill were quite similar except no weaving and finishing existed in the spinning mill. Total dust concentration was measured by area sampling. A total of 106 samples were obtained. The dust levels indicated in this paper were the arithmetic means of the time weighted average values for the locations sampled in each workplace.

RESULTS

Dust Concentration and Its Chemical Composition

The dust concentration in different jute processing areas is shown in Table I. Dust concentrations in spinning mills were higher than those in weaving factories The mixing, softening procedure produced very high levels of dust, and dusts in these areas contained high mineral material and high silica (13.3%–14.3%). Dust levels in other areas were lower than 5 mg/M^3 and contain low mineral material and less than 5% silica. After averaging the results of dust distribution from different workplaces, we found 65.1% of particles were under 5μm; 23.5% of particles were between 5.0 to 10.0μm; only 12.4% particles were larger than 10μm. This result indicated

Table I
Dust Concentration and Its Chemical Composition in Jute Mills

Procedures	Total dust (mg/M^3) weaving factory	Total dust (mg/M^3) spinning mill	Ash (%)	Silica (%)
mixing#*	35.6	53.6	50.9	14.3
softening#*	48.5	120.3	25.4	13.4
carding#*	4.0	6.8	12.6	6.2
spool#*	1.5	1.8	1.6	1.6
copping#	1.8	-	1.8	1.8
roving*	-	1.9	20.9	1.8
Spinning#*	4.9	8.6	8.3	1.1
copping*	-	20.4	5.8	1.4
winding*	-	0.9	12.2	1.3
weaving#	1.6	-	11.1	2.3
finishing#	2.2	-	5.8	1.5

#:manufacturing procedure in weaving factory
*:manufacturing procedure in spinning mill

that most jute dusts in this mill were inhalable.

Respiratory Symptoms

In order to find the chronic effect of jute dust exposure, we included many workers who had been employed more than 20 years or were ex-workers. This resulted in a difference in the age distribution between two groups. The exposed group had more workers who were over 50 years old. There were nearly 40% of workers who had been exposed to dust for more than 20 years. So, standardization method (chi square test for comparison of rates with inner distribution difference) was used to compare the respiratory symptoms between two groups. Figures 1 to 3 show the results of the comparison. Because few female smokers exited in both groups, comparison of the symptoms was only conducted in female nonsmokers. Prevalence of all the respiratory symptoms were higher in exposed groups than in control groups. Exposed workers had significantly higher prevalence of cough, chest tightness symptoms than control workers in both male smokers and nonsmokers groups. In exposed female nonsmokers, the prevalence of cough, bronchitis, chest tightness and dyspnea were also significantly higher when compared with those of control female nonsmokers. We also compared the prevalence of respiratory symptoms in smokers and nonsmokers. In exposed male, the prevalence of cough and bronchitis were significantly higher in smokers than those in nonsmokers ($X^2 = 6.09$, $P<0.05$; $X^2 = 5.54$, $P<0.05$). In control male workers, the smokers had significantly higher prevalence of cough compared with nonsmokers ($X^2 = 12.1$, $P<0.01$).

Lung Function

The abnormal of lung function was evaluated by the percentage of predicted value. Table II shows the results of the comparison of abnormal rates of FVC, $FEV_{1.0}$, $FEV_{1.0}$/FVC between the exposed workers and control workers. The abnormal rates of FVC, $FEV_{1.0}$ and $FEV_{1.0}$/FVC were significantly higher than those in exposed workers. Comparing with control workers, the exposed workers had increased 3.2% abnormal rate in FVC; 12.9% abnormal rate in $FEV_{1.0}$, 7.5% abnormal rate in $FEV_{1.0}$/FVC. 5.4% of exposed workers had severe abnormality of $FEV_{1.0}$.

Because smoking is an important factor in causing lung dysfunction, we used $FEV_{1.0}$ to analyze the effect of smoking on lung function. $FEV_{1.0}$ was selected since it is an important index to evaluate the permanent lung function injury due to vegetable dusts.[1] The comparison of abnormal of $FEV_{1.0}$ between male smokers and nonsmokers in exposed and control groups were shown in Table III. Odd ratios were calculated to analyze the contribution of smoking and dust exposure to abnormality of lung function. The results indicated both dust exposure and smoking would cause lung function loss, but dust exposure was much more effective than smoking. Dust exposure and smoking had combined effects in increasing abnormal rate of $FEV_{1.0}$.

DISCUSSION

Recently, more attention has been paid to the chronic effect of vegetable dust.[1,2,9] Some investigators have studied chronic effects of cotton, flax dusts.[9,10,11,12,13] They found permanent lung injury in cotton workers.[10,11,12] The permanent lung injury or loss of lung function may not necessarily come from "Monday" symptom and acute reversible lung function decrement.[2] In our study, we found jute dust exposure caused increased prevalence of caught, chest tightness in exposed male workers (both smokers and nonsmokers) and increased prevalence of caught, chest tightness, chronic bronchitis, dyspnea in female workers (nonsmokers). Among

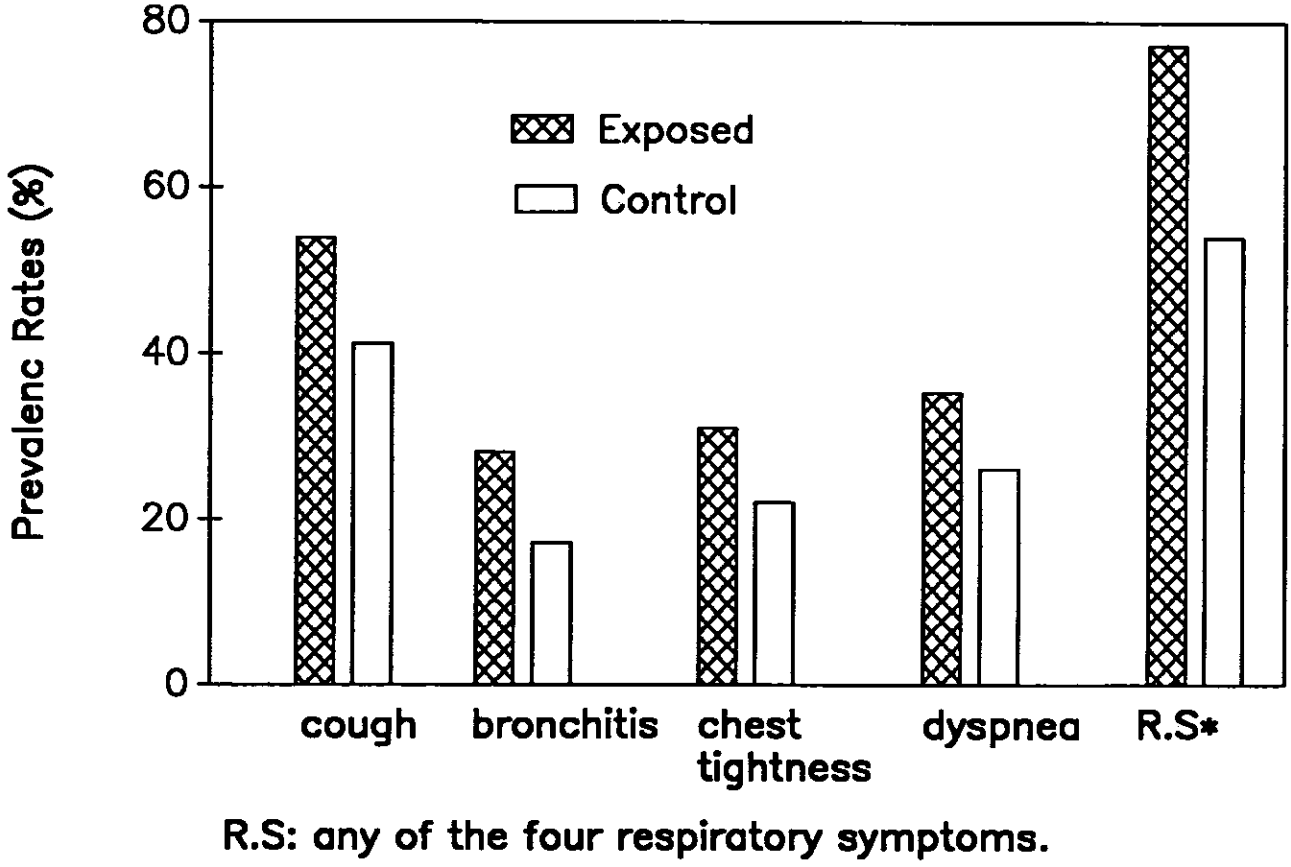

Figure 1. The prevalence of respiratory symptoms in male smokers.

Table II

Comparison of Rates of Abnormality of Percentage of Predicted Value of FVC, $FEV_{1.0}$, $FEV_{1.0}$/FVC between Exposed and Control Workers

Lung function	Percent predicted values	Exposed workers No.	Exposed workers %	Control workers No.	Control workers %	X^2	P
FVC	>0.80	331	93.5	356	96.7	4.1	<0.05
	<0.80	23	6.5	12	3.3		
$FEV_{1.0}$	>0.80	276	78.0	334	90.8	22.7	<0.01
	0.60-0.79	59	16.7	27	16.7		
	<0.60	19	5.4	7	1.9		
$FEV_{1.0}$/FVC	>0.75	328	89.8	358	97.3	26.1	<0.05
	<0.75	36	10.2	10	2.7		

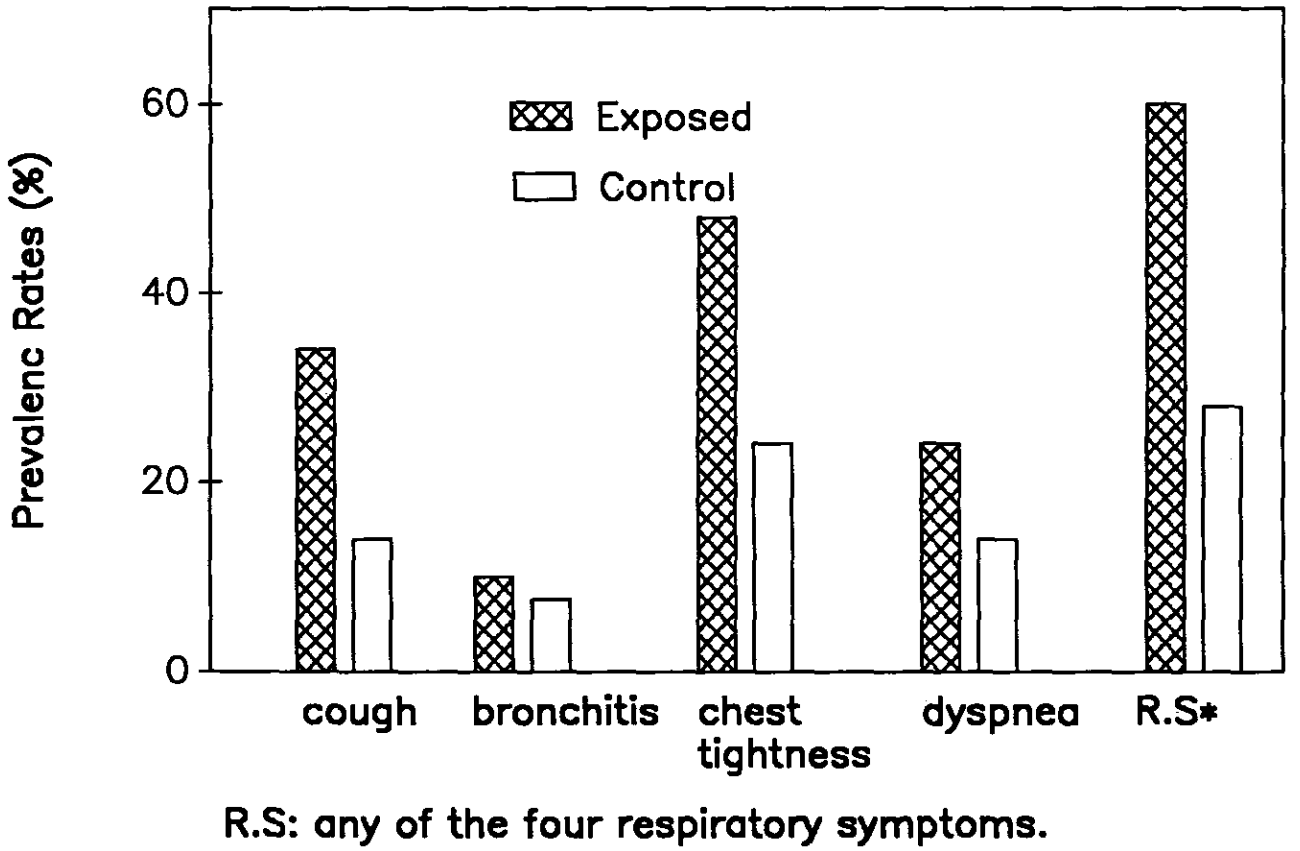

Figure 2. The prevalence of respiratory symptoms in male nonsmokers.

Table III

Contribution* of Dust Exposure and Smoking to Lung Dysfunction Expressed by Abnormal Rate of Percent of Predicted Value of $FEV_{1.0}$

Dust exposure	Smoke	Abnormal rate of $FEV_{1.0}$ <0.80	Abnormal rate of $FEV_{1.0}$ >0.80	Odd ratio (OR)
-	-	5	58	1.00
-	+	13	149	1.01
+	-	10	37	3.14
+	+	45	111	4.70

* $OR_{dust}+OR_{smoking}=4.15$ $OR_{dust+smoking}=4.70$
$OR_{dust+smoking}>OR_{dust}+OR_{smoking}$

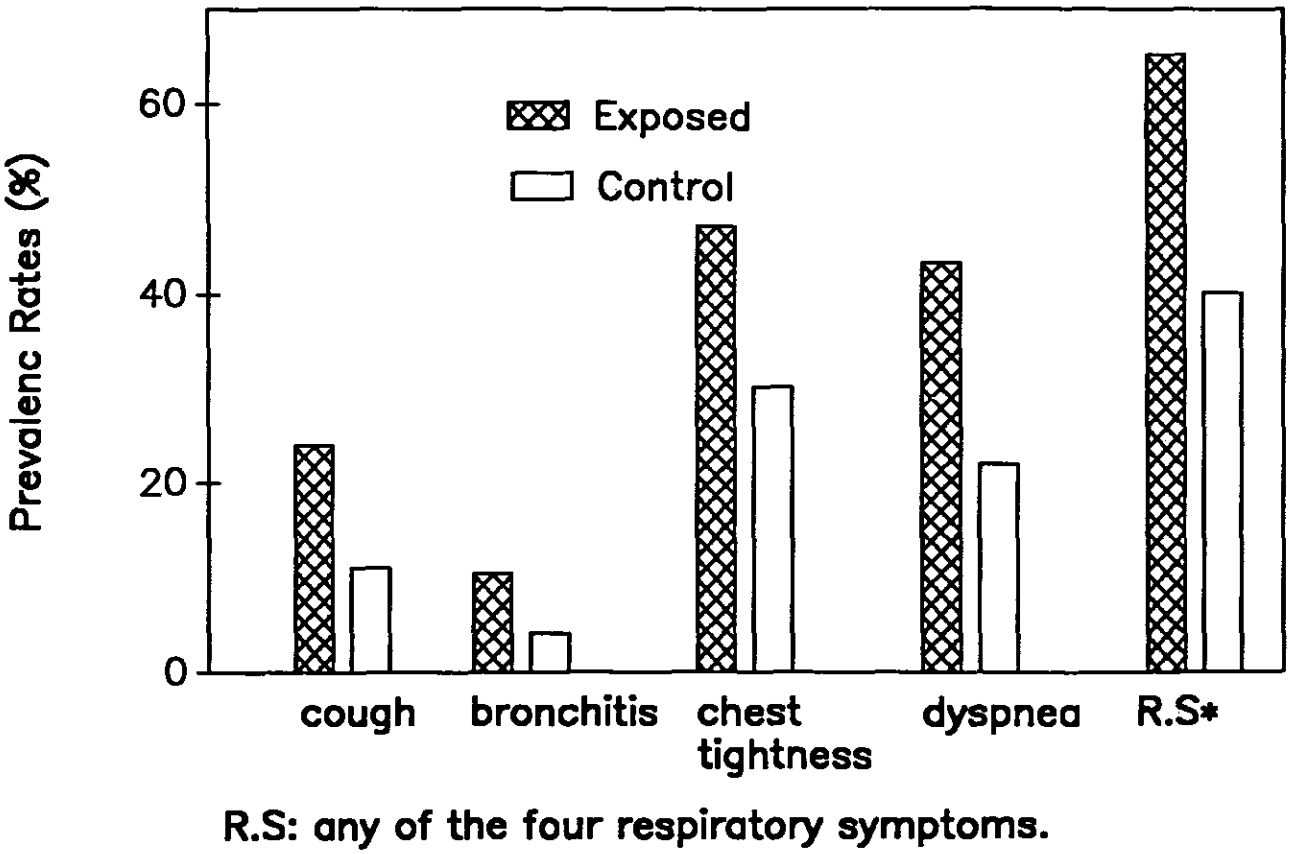

Figure 3. The prevalence of respiratory symptoms in female nonsmokers.

exposed workers, cough and chest tightness not only occurred on Monday, but also occurred in other working days. Smoking itself only caused a higher prevalence rate of cough in both exposed and control groups. With dust exposure, smoking caused a higher prevalence of chronic bronchitis. This means smoking was not the main cause of all these symptoms. The atypical chest tightness and chronic bronchitis were the main clinical symptoms in jute processing workers. There was no typical "Monday" symptom in our study. These findings were similar to the report from Ghawabi, E. L. et al.[6]

Valic, F. et al reported acute lung function loss in nonsmoking female jute workers.[7] Ghawabi et al, Gandevia and Milne found the acute decline of $FEV_{1.0}$ in the first working shift in jute processing workers.[6,8] We also found jute processing workers had significantly higher abnormal rates of FVC, $FEV_{1.0}$, $FEV_{1.0}$/FVC before the beginning of first working day. The abnormal rate of $FEV_{1.0}$ increased more than 12.9% and rate of severe abnormality of $FEV_{1.0}$ increased more than 3.5% in exposed workers when comparing with control workers. The reasons of difference of results between ours and Mair, A. et al may be due to higher dust levels in our study and different lung function index used. Our results indicated that there is an occupational lung disease problem in China jute industry.

Beck, G. J. et al reported cotton dust and smoking have combined effect in causing the lung function loss.[11] We had also found that jute dust and smoking has such an effect. Jute dust exposure was a main cause for abnormality of lung function, but smoking would increase the abnormal rate of lung function caused by dust exposure. We, therefore, concluded that the chronic lung injury in jute processing workers may be mainly due to high level and long duration of jute dust exposure. Our results of industrial hygiene investigation show that jute processing is a very dusty industry. The early steps of processing of jute, especially the mixing and softening procedures produced high levels of dust which contained considerable amounts of ash and silica. The results of high levels of dust in these areas was from manual operation, and high content of ash and silica were associated with earth or dirt on the surface of jute fiber. The other procedures also produced about 2 to 5 mg/M^3 dust and most of the dusts were inhalable. The concentration was also higher than the ACGIH recommendation for cotton dust. The jute processing workers, therefore, inhaled a considerable amount of dust, which may account for their lung injury.

The mechanisms of lung disease caused by vegetable dust are very complicated because dust in the workplace is complex. Mineral impurities, special chemical component of fiber and microorganisms are commonly believed to be main etiological factors. In our study, we found there were different mineral and silica contents in different workplaces. A few jute

processing workers were exposed to dust containing 10% to 15% silica, but most workers were exposed to dust containing less than 5% silica. We analyzed the relationships between the mineral content, silica content in dusts and respiratory symptoms and lung function, no relationship was found, all correlation coefficients were below 0.50. The chest X-ray examination of workers who had worked in high level dust areas in this mill for more than 20 years showed no diagnosable silicosis or pneumoconiosis.[14] In our study, there was no evidence that mineral and silica content in jute dust were important factors in jute dust induced lung injury. The mechanism of jute dust induced lung injury may be due to special chemical components of fiber or microorganism, or it may be simply a nonspecific respiratory irritant.[3] Further study is needed to better understand the mechanism of lung injury produced by jute dust.

We concluded that jute processing is a very dusty industry. Exposure to jute dusts caused significant increase in respiratory symptoms and significant increase of abnormal rate of FVC, $FEV_{1.0}$, $FEV_{1.0}$/FVC. Smoking had an additive effect in lung function injury.

REFERENCES

1. WHO.: *Recommended Health-based Occupational Exposure Limits for Selected Vegetable Dusts.* WHO Technical Report Series 684, Geneva (1983).
2. Rylander, R., Schilling, R.S.F., Pickerig, C.A.C., Dempsey, A.N., Jacobs, R.R.: Effect after Acute and Chronic Exposure to Cotton Dust: the Manchester Criteria. *Brit. J. Ind. Med.* 44:577-579 (1987).
3. Schilling, R.S.F.: Worldwide Problems of Byssinosis. *Chest. supplement* 79:3S-5S (1981).
4. Mair, A., Smith, D.H., Wilson, W.A., Lockhart, W.: Dust Diseases in Dundee Textile Workers. *Brit. J. Ind. Med.* 17:272-278 (1960).
5. Gilson, J.C., Stott, H., Hopwood, B.E.C., Roach, S.A., Mckeerrow, C.B., Schilling, R.S.F.: Byssinosis: The Acute Effect on Ventilatory Capacity of Dusts in Cotton Ginneries, Cotton, Sisal, and Jute Mills. *Brit. J. Ind. Med.* 19:9-18 (1962).
6. Ghawabi, E.L.S.H.: Respiratory Function and Symptom in Workers Exposed Simultaneously to Jute and Hemp. *Brit. J. Ind. Med.* 35:16-20 (1978).
7. Valic, F., Zusin, E.: A Comparative Study of Respiratory Function in Female Nonsmoking Cotton and Jute Workers. *Brit. J. Ind. Med.* 28:364-368 (1971).
8. Gandevia, B., Milne, J.: Ventilatory Capacity on Exposure to Jute Dust and the Relevance of Productive Cough and Smoking to the Response. *Brit. J. Ind. Med.* 22:187-195 (1965).
9. Schilling, R.S.F.: Long Term Respiratory Disability in Cotton and Flax Workers. *Lancet.* part 2:330 (1982).
10. Beck, G.C., Schacter, E.N.: The Evidence for Chronic Lung Disease in Cotton Textile Workers. *Am. Stat.* 37: 404-412 (1983).
11. Beck, G.J., Maunder, L.R.,Schachter, E. Neil.: Cotton Dust and Smoking Effects on Lung Function in Cotton Textile Workers. *Am. J. Epidemiol.* 119:33-43 (1984).
12. Elwood, P.C., Sweetnam, P.M., Bevan, C.: Respiratory Disability in Ex-cotton Workers. *Brit. J. Ind. Med.* 43:580-586 (1986).
13. Elwood, J.H., Elwood, P.C., Stanford, F., Chivers, A., Hey, Iris-Brewster, L., Sweetnam, P.M.: Respiratory Symptoms in Ex-flax Workers. *Brit. J. Ind. Med.* 43:300-306 (1986).
14. Chen, Z., Jiezhi, L., Zenlin, L.: Comparison of Chest X-ray and Lung Function Changes in Jute Processing Workers. (to be published)

RELATIONSHIP BETWEEN SERUM LIPID PEROXIDES AND SOME IMMUNOLOGICAL PARAMETERS IN SILICOSIS

E. TUFANOIU* • Silvia Gabor† • Ligia Bochisiu*

*County Hospital Deva

†Institute of Hygiene and Public Health, Cluj-Napoca, Romania

In various environmental conditions (xenobiotics, irradiation, hyperoxia), during oxido-reducing metabolic processes,[11,12,22] and in case of some pathologic processes with generation of circulating immune complexes or ischaemia,[1,19] activated reactive oxygen forms as superoxide, hydroxyl radicals, singlet oxygen and hydrogen peroxides are produced. These free radicals interact with all tissues, especially with cellular membrane polyunsaturated fatty acids, inducing by chain reactions lipid peroxide release (mainly alkoxy-RO• and peroxy-ROO• radicals), and derivate components as malondialdehyde (MDA), lipidic alcohols, lipofuscin.[2,5,9,12] The peroxidation of membrane lipids and the by-products of MDA type modify and/or destroy cellular membranes and cause impairment of biological functions and structures: enzyme inactivation, increased rigidity, polymerization and formation of cross linkings between various components (aminic groups of proteins, phospholipids, glycoproteins). In case that biochemical lesions are not reversible, the death of the cells occurs.[2,11]

Lipid peroxidation is involved in the pathogenesis of numerous lung diseases such as: certain forms of lung edema,[11,20,26] lung fibrosis,[15,18] lung cancer,[15,22] emphysema and bronchitis,[11,18] hyaline membrane disease,[4,24] and experimental silicosis.[13,14,16]

Up to certain limits the damaging effects of oxygen radicals are counteracted by a number of intracellular detoxifying agents, including the antioxidant defense enzyme systems: superoxide dismutase, catalase, glutathione peroxidase, glutathione S-transferases. A nonenzymatic defense equipment—vitamins A, E, C, thiol groups—is also capable of decreasing oxygen free radicals.[6,9,17]

On the other hand, involvement of immune and inflammatory systems in the fibrogenic response is now well documented; however, its precise role remains to be defined.[21] The extent to which immunological mechanisms are directly or indirectly involved in the silicotic fibrosis initiation and/or propagation is very unclear. Various non-specific alterations of immune functions, mainly augmentation of humoral immunity have been reported in silicotic patients.[7,10] Stimulation of immunoglobulin production in response to quartz might result from the effects of secreted by macrophages Interleukin-1, or from the activated helper T-lymphocytes.[8] Concomitant generation of reactive oxygen metabolites, as specific mediators released by stimulated inflammatory cells, represents one of the effector mechanisms in modulating immunologic responses.[10]

Most of the data that have been published concerning lipid peroxidation under dust action result from experimental studies. There is no report on lipid peroxide levels in silicotic patients. Therefore, the purpose of the present study was to investigate serum lipid peroxides in silicotic subjects. We attempted also to explore whether lipid peroxidation correlates with the humoral immune response.

MATERIAL AND METHODS

The investigation was carried out on 40 silicotic miners and on 40 healthy subjects, both groups having a matched-mean age. Serum lipid peroxides were measured by the formation of malondialdehyde, using thiobarbituric acid (TBA) method, and spectrophotometric readings.[25] The serum immunoglobulins (IgA, IgG, and IgM), and the complement were assayed with the simple radial immunodiffusion, by means of immunoplates supplied by the Cantacuziono Institute in Bucharest.

The results obtained on silicotics were compared to findings of control group by using Student's t-test. A correlation between lipid peroxide and immunoglobulin values was calculated.

RESULTS AND DISCUSSION

An increase of serum lipid peroxides in silicotic subjects compared to control group was noticed (Figure 1). The mean value in silicosis was 5.8 ± 1.6 nmol MDA/0.5ml serum versus 3.02 ± 1.02 nmol MDA/0.5ml serum of control group. The difference was of high significance ($p < 0.001$). The increase of lipid peroxidation is not surprising as the conditions exist in favour of forming them through the persistence of the antigenic stimulus. This stimulus induces a continuous release of oxygen activated metabolites, with the formation of peroxides, especially hydroperoxides and leukotrienes with chemotactic effect,[9] emphasizing the inflammation, and further generating larger influx of oxygen radicals. There is worth mentioning also the presence of the iscaemic process which strengthens along with the disease progression, and which may have two consequences: (1) the conversion of xanthine dehydrogenase into xanthine oxydase,[19] and, (2) the diminution of the reduced glutathione which acts in cooperation with glutathione S-transferases.[5,11]

The assay of immunoglobulins revealed a significant increase ($p < 0.001$) of IgG component when compared to normal values found in healthy control group (Figure 2). The mean level of IgG in silicosis was 270 ± 59.75 UI/ml serum, while in control group the mean level reached only 150 ± 50 UI/ml serum. No differences of IgA and IgM globulins as well as of serum complement were noticed between silicotic and control groups. A positive correlation, shown in Figure 3, was registered between the levels of serum lipid peroxides and those of the IgG. This finding could be explained by the fact that biochemical abnormalities and lung tissue modifications led to non-self structures with immunogene properties. The possibility of further perpetuation of this mechanism induced by chain release of free radicals exists in conditions of persistent antigenic stimulus exerted by quartz activated inflammatory cells. This could be the "primum movens" in the starting of autoimmune mechanisms.

The involvement of oxygen free radicals in collagen accumulation by non-immune mechanisms is also pertinent. This effect may occur through the nonenzymatic hydroxylation of proline to hydroxyproline with the edification of hydrogen bindings among peptidic chains and their association in tricatenary helicoid structures.[3,21] Subsequent increased collagen synthesis and fibrotic nodule results. The findings that the anticancer drugs such as bleomycine, antracyclines and some nytrofuranes produce oxygen radicals, inducers of fibrosis,[11,21,23] support the hypothesis that a same mechanism may also operate in silicotic fibrosis.

In conclusion, this study confirms that free radical-induced lipid peroxidation might be of particular significance in the development of silicosis in humans, and, thus, could hold a perspective to new therapeutic measures.

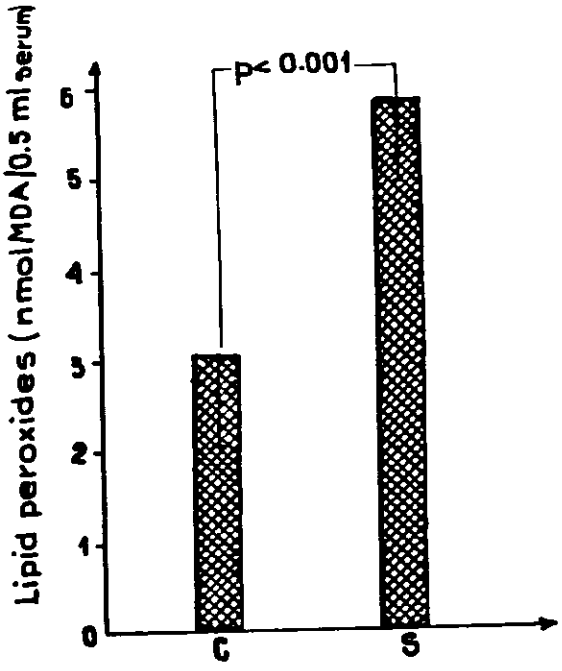

Figure 1. Serum lipid peroxides in silicotic patients.

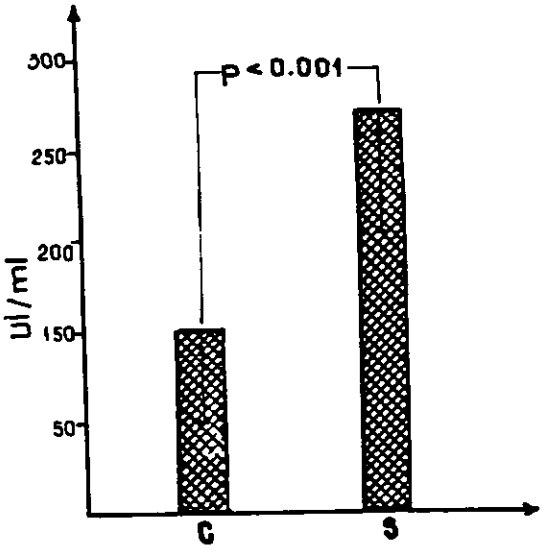

Figure 2. Serum immunoglobulin IgG in silicotic patients.

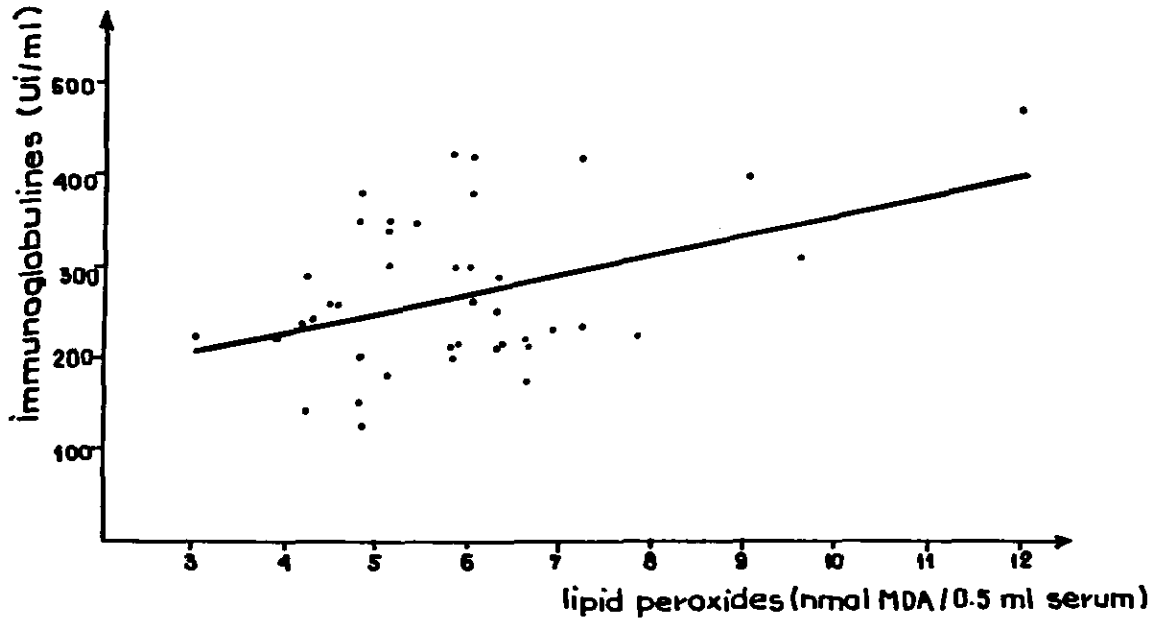

Figure 3. Correlation between serum lipid peroxides and immunoglobulin IgG in silicotic patients, $R=0.444$, $p < 0.01$.

REFERENCES

1. Abramson, S., Weissmann, G.,: The Release of Inflammatory Mediators from Neutrophils. *Ricer. Clin. Lab.* 2:91-99 (1981).
2. Armstrong, D.: Free Radical Involvement in the Formation of Lipopigments. *Free Radicals in Molecular Biology, Aging and Disease.* pp.129-141, Armstrong, D. et al eds. Raven Press, New York (1984).
3. Borel, J.P.: Radicaux Libres Oxygénés, Tissu Conjonctif et Inflammation. *Path. Biol.* 1:8-10 (1983).
4. Brown, R.E., Craver, R., Drake, M.: Lipid Peroxidation and Pulmonary Hyaline Membranes of the New Born. *Ann. Clin. Lab.* 1:25-29 (1981).
5. Burk, F.R.: Glutathione-Dependent Protection by Rat Liver Microsomal Protein Against Lipid Peroxidation. *Biochim. Biophys. Acta* 757:21-28 (1983).
6. Capel, I.D., David, L., Helen, M., Dorre, L.L.: Vitamin E Retards the Lipoperoxidation Resulting from Anticancer Drug Administration. *Anticancer Res.* 3:59-62 (1983).
7. Cocarla, A., Gabor, S., Milea, M., Suciu, I.: Serum Immunoglobulines in Workers Exposed to Silicogenic Risk with Tuberculin-Negative Test and Hyperergia. *J. Hyg. Epidemiol. Microbiol. Immunol.* 4:374-380 (1977).
8. Davis, G.S.: The Pathogenesis of Silicosis. State of the Art. *Chest* 89:166S-169S (1986).
9. DelMaestro, R.F.: Free Radical Injury During Inflammation. *Free Radicals in Molecular Biology, Aging and Disease.* pp. 87-101. Armstrong, D. et al eds. Raven Press, New York (1984).
10. Fantone, J.C., Feltner, D.E., Brieland, J.K., Ward, P.A.: Phagocytic Cell-Derived Inflammatory Mediators and Lung Disease. *Chest* 91:428-435 (1987).
11. Frank, L.: Superoxide Dismutase and Lung Toxicity. *Trends Pharmacol.* 3:124-128 (1983).
12. Freeman, A.B., Crapo, J.D.: Free Radicals and Tissue Injury. *Lab. Invest.* 5:412-426 (1982).
13. Gabor, S., Frits, T., Anca, Z.: Taux des Lipoperoxides dans le Poumons et le Myocarde Droit dans la Silicose Experimentale chez le rat. *Arch. Mal. Prof.* 32:553-558 (1974).
14. Gabor, S., Anca, Z., Zugravu, E., Ciugudeanu, M.: In Vitro and Vivo Quartz-Induced Lipid Peroxidation. *The In Vitro Effects of Mineral Dusts.* pp.131-137, R.C. Brown, M. Chamberlain, R. Davies, I.P. Gormley eds. Academic Press. London (1980).
15. Gulumian, M., Sardianos, F., Kilroe-Smith, T., Ockerse, G.: Lipid Peroxidation in Microsomes Induced by Crocidolite Fibers. *Chem. Biol. Interact.* 44:111-118 (1983).
16. Gupta, G.S., Kaw, J.L.: Formation of Lipid Peroxides in the Subcellular Fractions of Silicotic Lungs in Rats. *Eur. Respir. Dis.* 63:183-187 (1982).
17. Jenkins, S.G., Lawrence, R.A., Tucker, W.Y.: Glutathione Peroxidase, Superoxide Dismutase, and Glutathione S-Transferase Activities in Human Lungs. *Am. Rev. Respir. Dis.* 130:302-304 (1984).
18. Kopferschmitt, J., Ledig, J.M., Jaeger, A., Sauder, Ph., Warter, A., Ziessel, M., Mantz, J.M.: Variations de la Superoxyde Dismutase Pulmonaire en Pathologie Humaine. *La Presse Méd.* 12:46 (1983).
19. McCord, M.J.: Oxygen-Derived Free Radicals in Postischaemic Tissue Injury. *New Engl. J. Med.* 3:159-163 (1985).
20. Parker, J.C., Martin, D.J., Rutili, G., McCord, M.J., Taylor, A.E.: Prevention of Free Radical Mediated Vascular Permeability Increases in Lung Using Superoxide Dismutase. *Chest* 83:5-53s (1983).
21. Phan, S.H.: Fibrotic Mechanisms in Lung Disease. *Handbook of Inflammation. Immunology of Inflammation.*, vol. 4, pp. 121-162. P.A. Ward ed., Elsevier, Amsterdam-New York-Oxford (1986).
22. Pryor, W.A.: Free Radical Biology: Xenobiotics, Cancer, and Aging. *Ann. New York Acad. Sci.* 227:1-21 (1982).
23. Revis, N.W., Marusic, N.: Glutathione Peroxidase Activity and Selenium Concentration in the Hearth of Doxorubicin-Treated Rabbits. *J. Molec. Cellul. Cardiol.* 10:945-951 (1978).
24. Rosenfeld, W., Evans, H., Jhaveri, R., Moanie, H., Vohra, K., Georgatos, E., Salazar, J.D.: Safety and Plasma Concentration of Bovine Superoxide Dismutase Administered to Human Premature Infants. *Rev. Pharmacol. Ther.* 5:151-161 (1982).
25. Satoh, K.: Serum Lipid Peroxide in Cerebrovascular Disorders Determined by a New Colorimetric Method. *Clin. Chim. Acta* 90:37-43 (1978).
26. Taylor, A.E., Martin, D., Parker, J.C.: The Effects of Oxygen Radicals on Pulmonary Edema Formation. *Surgery* 3:443-438 (1983).

RAMAN SPECTROSCOPIC STUDIES ON THE MECHANISMS OF MEMBRANE DAMAGE INDUCED BY QUARTZ AND THE PROTECTIVE EFFECT OF ALUMINIUM CITRATE

CHENG J. CAO,* M.D. • Shi J. Liu,* M.D. • Ke C. Lin,† Ph.D.

*Dept. of Occupational Health, School of Public Health

†Dept. of Biophysics, School of Basic Medicine Beijing Medical University, 100083, Beijing, China

ABSTRACT

The molecular mechanisms of membrane damage induced by quartz and the antagonistic effect of aluminium citrate (Al citrate) against its toxicity were studied with liposomes by laser Raman spectroscopy. Liposomes under the action of quartz represented a Raman spectrum, in which the choline band shifts about 2-3 cm^{-1} toward the lower frequency and its intensity reduces, while its width increases; the intensity ratio of 1127 cm^{-1} to 1093 cm^{-1} bands decreases, so does the intensity ratio of 2883 cm^{-1} to 2847 cm^{-1} bands. These results show that quartz can react on phospholipids and form a stable complex with their polar head groups, $-N+(CH_3)_3$. The change of hydrocarbon chain conformation is caused by the interaction of quartz with the heads of phospholipids and deformation of liposomes. However, the similar change of choline groups cannot be found in Raman spectrum of liposomes under quartz pretreated with Al citrate or $AlCl_3$, and the order of hydrocarbon chain remains constant. The fact indicates further that Al citrate can exhibit its protective effect on membranes through the action of Al on the surface of quartz particles so that the direct interaction of quartz with lipidic molecules was blocked. As for titanium dioxide, it acts on liposomes too weak to cause any change of Raman spectrum, which is consistent with its weaker damage to the membranes.

INTRODUCTION

The injurious effect of quartz on cell membranes plays an important role in the pathogenic mechanism of silicosis. The significant effects of quartz on the functional and structural properties, such as fluidity, permeability, "water structure" and surface charge, of cell membranes as well as liposomes and the antagonistic effects of Al citrate were demonstrated in a series of our earlier experiments.[1-4] However, their molecular mechanisms remain to be clarified. For this reason, the studies of interactions of quartz, titanium dioxide and Al citrate with liposomes were carried out by laser Raman spectroscopy.

The use of Raman spectroscopy as a tool for research on the function and structure of membranes is a rapidly growing field. The quantitative molecular interpretations of the spectral events accompanying conformational alternations can be studied by this technique. Liposomes are often taken as a model for biomembranes because lipids in biomembranes are usually in a bilayer form. In the present study, we used dipalmitoyl-phosphatidylcholine (DPPC) to prepare liposomes due to its definite assignment of Raman bands.

In light of the finding that the injurious effect of quartz on membranes was lowered markedly by the pretreatment of these particles with Al citrate,[1-4] the present study was concentrated on the observations of Raman spectral effect of this pretreatment to elucidate its pharmacology.

MATERIALS AND METHODS

1. Quartz (99% pure) was supplied by Hygiene Institute of Chinese Prophylatic Medical Center. Titanium dioxide with a similar pure and size was obtained from Beijing Medical Chemical Factory. Al citrate with Al of 9.26% was supplied by Pharmaceutical Factory of Beijing Medical University. Quartz particles were pretreated with Al citrate or $AlCl_3$ using the method reported by Zou, T.T. et al.[5-6] DPPC was purchased from Sigma. Liposomes were prepared at the concentration of 100 mg/ml using the method described previously.

2. Raman spectra were obtained with Trimonochrometer Raman Spectrometer Model YJT-800. The 5145 A line of the laser was selected as excitation. The used power was 400-500 mw. Spectral slit width and scanning velocity were 800 μm and 1 cm^{-1}/sec, respectively. The computer was used to average signal, which was accumulated about 4-6 times. Spectra were not smoothed and only baseline was modified appropriately. Variance of sharp peaks were no more than 2 cm^{-1}. Qaulitative and quantitative analysis of the data were evaluated by the intensity ratio and order parameters to avoid interference.

RESULTS

C-N Band

715 cm^{-1} band in DPPC is the C-N stretching mode. The 1259 cm^{-1} bands are assigned to twisting and bending vibration modes of C-H, respectively, which are often utilized as an internal standard of C-N bands due to their high intensity and their insensitivity to environmental factors.

As shown in Table I and Figure 1, the 715 cm^{-1} band shifted about 2-3 cm^{-1} toward the lower frequency and its intensity was decreased markedly in DPPC+quartz group. As compared to DPPC control group, the intensity ratio of 715 cm^{-1} band to 1295 cm^{-1} or 1437 cm^{-1} band was reduced by 26.6% and 30.5% in 0.5 mg of quartz, respectively, while the reductions were more significant, that is 31.6% and 40.3%, respectively. Figure 2, the enlarged C-N band, illustrates clearly that the width of C-N peak was increased in DPPC+quartz group. However, these changes of C-N band caused by quartz almost disappeared by the pretreatment of quartz particles with Al citrate or $AlCl_3$. (Table I and Figures 1-2)

C-C Skeletal Structure

The skeletal optical modes in 1000-1200 cm^{-1} region include generally C-C and P-O stretching vibrations. Three principal bands to be used to estimate the intrachain order exist in this region. Figure 1 represents the Raman spectra in 1040-1150 cm^{-1} region of DPPC groups and its treated groups. The data listed in Table II show that quartz can decrease the intensity ratio of 1127 cm^{-1} to 1093 cm^{-1} bands and the intrachain parameter S_T, particularly in its 1.0 mg group, S_T was reduced by 21.6% compared to DPPC control. Whereas the pretreatment of Al citrate or $AlCl_3$ for quartz can partly reverse the effect of quartz, S_T tended to go uptowards. In contrast to quartz, these parameters did not change significantly in DPPC+titanium dioxide group, which means titanium dioxide cannot interfere with C-C skeletal structure of phospholipid membranes.

Table I
The Shift of C-N Band and Its Intensity Ratio
to 1295 or 1437 Bands

Group	C-N cm^{-1}	I CN /I 1295 cm^{-1}		I CN /I 1437 cm^{-1}	
	$\bar{x}$	$\bar{x}$	%	$\bar{x}$	%
control	715.2	0.79	100.0	0.62	100.0
quartz (0.5mg)	713.2	0.58	73.4	0.43	69.5
(1.0mg)	712.4	0.54	68.4	0.37	59.7
quartz pretreated with Al citrate	715.2	0.79	100.0	0.57	91.9
quartz pretreated with $AlCl_3$	714.6	0.78	98.7	0.58	93.5
titanium dioxide	714.8	0.80	101.3	0.61	98.4

The doses of the pretreated quartz and titanium dioxide were 1.0 mg.

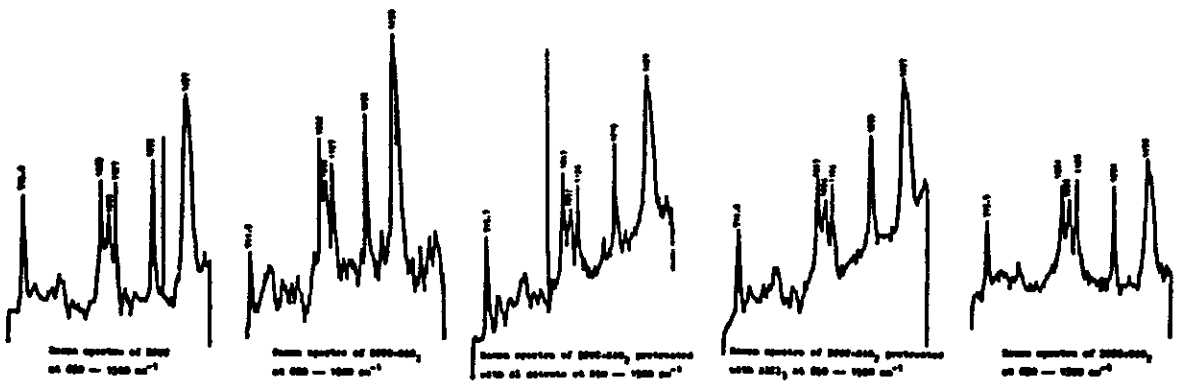

Figure 1.

C-H Stretching Vibration

The C-H stretching in 2800-2900 cm^{-1} region includes mainly the methylene symmetric stretch (2847 cm^{-1}) and asymmetric stretch (2882 cm^{-1}), which are used to evaluate the lateral packing order.

It can be seen from Table III and Figure 3 that the intensity ratio of 2882 cm^{-1} to 2847 cm^{-1} bands and the lateral order parameter S_L were lowered largely in two doses of quartz. Of interest, the intensity ratio and S_L values were enhanced markedly in both these pretreated groups, indicating that the interchain packing order was recovered partly. Likewise, there was no alternation in Raman spectrum in 2800-2900 cm^{-1} region of DPPC+titanium dioxide group. These findings suggest that titanium dioxide acted on liposomes weakly.

DISCUSSION

Raman spectra of lipids reflect mainly the vibrations of polar head group and C-H bonds. The 715 cm^{-1} band is the C-N symmetric stretching vibration mode. C-N group was even taken as an internal standard because it is constant and does not appear in the difference spectra.[7] It will be, therefore, a matter of great interest once the group has changed. The frequency of C-N band shifted, its intensity decreased and its width enlarged in DPPC under the action of quartz. This fact indicates that C-N group is an important site with which quartz interacts in membranes.

There a number of hydroxy groups on the surface of hydrated quartz, and silicic acid can be hydrolyzed partly to $HSiO_3^-$ in pH between neutral and alkaline due to its PK_1.[10-1] Whereas phospholipids of membranes rich in choline groups charged positively, which seems to provide $HSiO_3^-$ with a "target group," and a potential polar or ionic bond between N and O may be formed, resulting in their electrostatic and hydrophilic interactions.

The distinct changes of C-N band in Raman spectrum implicate that this binding is rather tight. According to this, it is explained why quartz can alter electrophoretic behaviour of macrophages and increase their negative charge density.[3] Also, the unhydrolyzed –OH groups of quartz surface form probably a hydrogen bond with $> P_2^-$ of phospholipid. On the other hand, deformation of liposomes to fit the globular surface of quartz particles may produce many binding sites

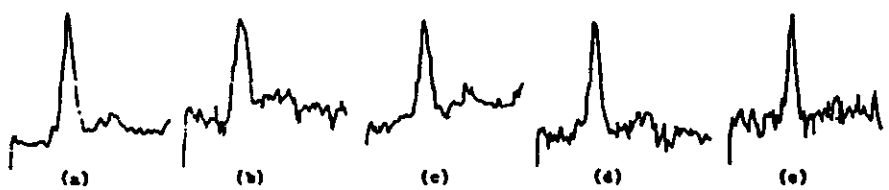

Figure 2. The enlarged C-N Raman band of DPPC (a), DPPC+SiO_2 (b), DPPC+SiO_2 pretreated with Al citrate (c), DPPC+SiO_2 pretreated with $AlCl_3$ (d), and DPPC+TiO_2(e).

Table II

The Intensity Ratio of 1127 to 1093 Bands and Order Parameter (S_T)

Groups	I 1127 cm^{-} /I 1093 cm^{-}	S_T	
	$\bar{X}$	$\bar{X}$	%
Control	1.36	0.74	100.0
quartz (0.5 mg)	1.24	0.68	91.9
(1.0 mg)	1.07	0.58	78.4
quartz pretreated with Al citrate	1.14	0.62	83.8
quartz pretreated with $AlCl_3$	1.17	0.64	86.5
titanium dioxide	1.39	0.76	102.7

The doses of the pretreated quartz and titanium dioxide were 1.0 mg.

Table III
The Intensity Ratio of 2882 to 2847 Band and Order Parameter (S_L)

Groups	I 2882 cm^{-1} /I 2847 cm^{-1}	S_L	
	$\bar{x}$	$\bar{x}$	%
Control	1.04	0.23	100.0
quartz (0.5 mg)	0.87	0.11	47.8
(1.0 mg)	0.90	0.13	56.5
quartz pretreated with Al citrate	1.02	0.21	91.3
quartz pretreated with $AlCl_3$	1.03	0.22	95.7
titanium dioxide	1.04	0.23	100.0

The doses of the pretreated quartz and titanium dioxide were 1.0 mg.

Figure 3. Raman spectra of DPPC (a), DPPC+SiO_2 (b), DPPC+SiO_2 pretreated with Al citrate (c), DPPC and SiO_2 pretreated with $AlCl_3$ (d), and DPPC+TiO_2 (e) at 2800–2900 cm^{-1}.

to force quartz and liposomes to form a tight complex. A good evidence for this is larger changes of bands at 2800-2900 cm^{-1} caused by quartz than that at 1040-1150 cm^{-1}.

The interaction of quartz with polar head group triggered a series of alternations of hydrocarbon chains. Membrane skeletal optical mode exists in 1000-1150 cm^{-1} region in Raman spectrum and is quite sensitive to the configuration of C-C bond. 1062 cm^1 and 1127 cm^{-1} bands are originated primarily from all-trans C-C stretching vibration, resulting in a zigzag chain on a plane, whereas 1093 cm^{-1} broad band is contributed by the Gauche vibration, which alters intrachain to a more disorder state. In general, information about the intrachain order and its molecular motion regulation may be obtained from the intensity rato of I1127 cm^{-1}/I1093 cm^{-1} and order parameter S_T.[7] The decreases in this intensity ratio and S_T resulting from the action of quartz on liposomes indicate a loss in the number of the trans isomers and an abnormal increase in the number of the Gauche isomers, leading the decreased intrachain order.[8]

The C-H vibration at high frequency region of 2800-2900 cm^{-1} is susceptible to the environmental factors and the direction of C-H chain. The intensity ratio of I2882 cm^{-1}/I2847 cm^{-1} and order parameter S_L are usually used to estimate the interchain order and its lateral molecular motion pattern.[7] The decrease of this intensity ratio and S_L induced by Quartz show that the lateral packing order was interfered simutaneously.

The molecular dynamic mechanism postulated in this paper was supported by the comparative studies of titanium dioxide and quartz pretreated with Al citrate or $AlCl_3$. It has been demonstrated that the affinity of titanium dioxide for quatenary ammonium group and Al^{3+} is much lower than quartz,[6-9] which is related to its hydration ability. Furthermore, titanic acid is so much weaker an acid than silicic acid that it is difficult to be hydrolyzed and to bind with C-N group, and also its ability to form hydrogen bond with $> P_2^-$ group is not as high as quartz. That is why titanium dioxide acts weakly on liposomes and no change of Raman spectrum could be found. It is more important that this is consistent with its weak cytotoxicity and its weak effects on cell membranes.

In light of the antagonistic effect of the pretreatment way against membrane damage by quartz, the present paper

centered on the observations of Raman spectroscopic effects of DPPC under the action of quartz particles pretreated with Al citrate or $AlCl_3$.

The results show that the changes of the main bands in the Raman spectra are very similar between the two pretreated groups. The frequency, intensity ratio and peak shape of C-N band were almost recovered to the control level. The intensity ratio of I2882 cm^{-1}/I2847 cm^{-1} and S_L went up markedly and closed to the control level. Whereas the intensity ratio of I1127 cm^{-1}/I1093 cm^{-1} and S_T were recovered only partly, indicating that the molecular degree of intrachain remained partly in the disorder. It seems therefore logical that Al citrate was unable to completely recover the effects of quartz on cell membranes, such as fluidity and permeability, to the control level. Moreover, it has been found that Al citrate did not alone affect Raman spectrum of DPPC in our preliminary experiment. So it is obvious that the effective component by which Al citrate exerts its phamacological effect is Al itself through the action on the surface of quartz particles.

REFERENCES

1. Cao, C.J.: Investigation of the Effects of Quartz and Aluminium Citrate on Fluidity of Artificial Membranes. *J. Chin. Ind. Hyg. & Occup. Dis.* 3:140 (1983).
2. Cao, C.J.: The Effect of Aluminium Citrate on Permeability of Macrophage Membranes to K+ Caused by Quartz. *Biochem. Biophys.* 1:39 (1985).
3. Cao, C.J.: The Effects of Quartz and Titanium Dioxide on Electrophoretic Mobility of Guinea Pig Alveolus Macrophages. *J. Chin. Ind. Hyg. & Occup. Dis.* 3:137 (1985).
4. Cao, C.J., Liu, S.J., Lin, K.C.: The Effects of Quartz and Aluminium Citrate on Membrane-bound Water of Erythrocytes. *Acta Biophys. Sinica.* 2:136 (1986).
5. Zou, T.T.: In Vitro Study of the Preventive Effect of Aluminium Citrate Against the Cytotoxicity of Quartz. *Matell. Ind. Hyg.* 6:246 (1982).
6. Cao, C.J.: The Effects of Aluminium Citrate on Electrokinetic Potential on the Surface of Quartz and Titanium Dioxide Particles. *J. Chin. Preven. Med.* 3:143 (1985).
7. Gaber, B.P., Peticolas, W.I.: On the Quantatitive Interpretation of Biomembrane Structure by Raman Spectroscopy. *Biochem. Biophys. Acta* 465:260 (1977).
8. Anthony, T. Tu: *Raman Spectroscopy in Biology.* pp. 187. A Wiley Interscience Publications, USA (1982).
9. Depass, J., et al: Comparison between Two Hypothesis about the Physicochemical Basis of the Toxicity of Silica. *J. Colloid Interface Sci.* 60:416 (1977).

STUDY OF FIBROGENIC EFFECTS OF SLAG CEMENT AND ITS RAW MATERIALS ON RAT LUNG

YANG MEIYU • Zhang Jifang • Zhao Xiuqing • Xu Guihua • Fu Bo

Shenyang Research Institute of Industrial Hygiene and Occupational Diseases, Shenyang, P.R. China

ABSTRACT

The fibrogenic effects of slag cement and its raw materials on rat lung and their effects on the survival rate of alveolar macrophages in vitro were studied. Seven groups were experimented: slag cement, raw material, ripe material, iron, slag, quartz and control group. 50 mg each of the above mentioned prepared dusts particulates was injected intratracheally into each rat. All rats were killed at an interval of 1, 3, 6 and 12 months. The wet/dry weights of the lung and collagen content of the lung were measured. The histopathological findings of the rat lungs and hilar lymphnodes were observed. The results showed that the raw and ripe materials caused the slight interstitial thickening and an increase of reticulin fibre while slag cement and iron induced an increase of slight collagen fibre, and in case of slag an increase of more collagen fibre was found. The results showed the fibrogenic effect of these dusts in vivo were in concordance with the toxicities of these dusts in vitro.

No Paper provided.

FEATURES OF CALCIFIED SILICOSIS AND ITS PROGNOSIS

ZHAO JINDUO • Wang Mingqui • Yang Meiyu • Liu Jingde • Win Xiuyun

Shenyang Research Institute of Industrial Hygiene and Occupational Diseases, Shenyang, P.R. China

ABSTRACT

Calcification of silicotic nodules is a special appearance in the development of some patients with silicosis. Because it occurs on the basis of silicotic lesions, so the site and extent of the calcification are in accordance with that of silicotic opacities. The sharply demarcated calcification became denser year by year, and the center of the small opacities were denser than their periphery. Coexistence of calcification of nodules and eggshell calcification of hilar lymphnodes usually concurred, and it is helpful to diagnosis. At autopsy, lung tissue was examined by polarizing microscope, electron probe and EDXA examination and results showed much of silica particles blocked in the calcified areas of the nodules. This might mean retention of particles in the calcified areas, thus, they could not be phagocytosed and transported by phagocytes to other areas, preventing the continuous tissue damage by particles. Therefore, the progress of the silicosis can be prevented with better prognosis. It is reasonable that the calcification of the silicotic nodules is an inactive phase and self-protection process of the silicosis.

No Paper provided.

DEVELOPMENT OF A NEW PERSONAL EXPOSURE MEASUREMENT SYSTEM CONSIDERING PULMONARY VENTILATION

TOSHIAKI HIGASHI,* M.D. • Toshihiko Satoh,† M.D. • Haruhiko Sakurai,† M.D., M.P.H. • Yasuhiko Baba,* M.D.

*University of Occupational and Environmental Health, JAPAN, Institute of Industrial Ecological Sciences, Kita-Kyushu, Japan

†Keio University, School of Medicine, Tokyo, Japan

ABSTRACT

The pulmonary ventilation is a critical factor for determining the intake of airborne pollutants. However, the present widely used monitoring for the evaluation of occupational exposures tends to ignore it. We have developed a monitor on experimental basis (HMR-3) with the function of measuring the real-time pulmonary ventilation in order to evaluate the actual exposure level, and presented it at ICOH, Sydney in 1987. On the findings obtained by HMR-3, we developed an improved device (DEM-1) which is sufficient for practical use in size and function.

DEM-1 system consists of four components. (1) Sensors for heart rate, for ambient dust concentration (mini-RAM), for body and environmental temperature, and for acceleration, (2) the data-logger which collects and inputs the data into IC-card, (3) the IC-card reader for the personal computer, (4) soft-wares for data processing. In this system, real-time pulmonary ventilation volume is predicted from average heart rate every 30 seconds using a conversion formula which includes the rate of change in heart rate, age, height and weight for each subject as explanatory variables.

Furthermore, DEM-1 has the following advantages. (1) By replacing the IC-card, the data-logger can be used continuously. (2) Capable of displaying the level of movement by acceleration sensor simultaneously, it is helpful for separately determining the degree of occupational hazards in each working unit.

INTRODUCTION

Exposure evaluation is indispensable for assessing the risk of airborne dusts in the workplace. Presently, when determining the level of individual exposure to airborne dusts, measurements are made by taking a sample from breathing zone. Those methods, however, do not take into account the level of physical exertion during exposure. Physical activity is known to increase pulmonary ventilation by about 10 times the level at rest.[1,2] Increased pulmonary ventilation causes an increment in the uptake of respirable dusts and affects the amount deposited.[3]

Thus, measurement of pulmonary ventilation, as well as the air concentration of airborne dusts, could seem to provide highly useful data in evaluating exposure. We have developed an instrument on experimental basis (HMR-3) for measuring exposure to air pollutants that continuously measures the concentration of air pollutants and the ventilation volume simultaneously, and presented it at ICOH, Sydney in 1987.[4] In this system, real-time pulmonary ventilation volume is predicted from average heart rate every 30 seconds using a conversion formula which includes the rate of change in heart rate, age, height and weight for each subject as explanatory variables. On the findings obtained by HMR-3, we developed an improved device (DEM-1) which is sufficient for practical use in size and function.

METHODS

Description of the System

Figure 1 shows the system outlines of the device (DEM-1). DEM-1 system consists of four components. 1) Sensors for heart rate, for ambient dust concentration, for body and ambient temperature, and for acceleration, 2) the data-logger which collects and inputs the data into IC-cards, 3) the IC-card reader for the personal computer, 4) soft-wares for data processing.

Dust sensor: This is a mini RAM, a small-sized dust measuring device manufactured by MIE, U.S.A., which measures mass concentrations by a light scatter detector.

Heart rate sensor: Electrodes Vitrode G-80 manufactured by Nihon Kohden Co. is used. The mean of the R-R intervals in a 30-second ECG recording represents the heart rate.

Accelerometer: An accelerometer (MT-3; Nihon Kohden Co.) that picks up changes in the intensity or the form of work

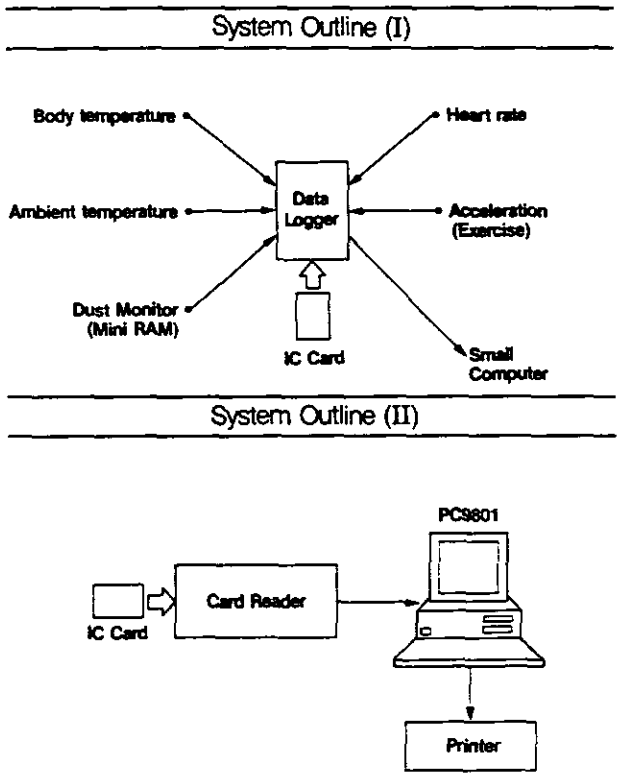

Figure 1. Essential components of DEM-1 and flow chart of data processing.

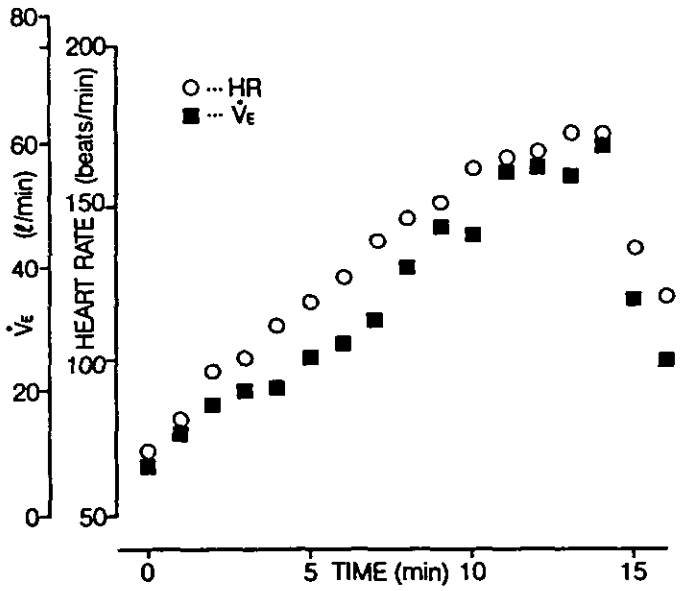

Figure 2. Typical HR response and $\dot{V}_E$ during graded exercise test using a treadmill.

is used as a sensor for physical activity.

Thermo sensor: This body and ambient temperature sensor provides additional ambient data on workers.

Data-logger: Analogue-data output from each sensor are A/D converted by the data-logger and recorded on the IC-card. The data-logger is attached to each worker by an exclusive belt. The measuring time, ID number, measuring channels are input by the keybord on the surface of data-logger.

IC-card: Digitalized data are recorded on the IC-card, read into the computer by the card reader and processed. Since the IC-card has a memory capacity of 128 K bit and can store data collected during 10 hours, data in all channels are recorded at intervals of 30 seconds.

Card reader: Data recorded on the IC card are recorded into a floppy disk by the card reader connected to the computer.

Personal computer: The hardware (PC-9801, NEC, Japan) includes dual floppy disk drives, color video monitor and color printer as options.

Laboratory Testing of DEM-1 System

For determining the regression equation between the ventilation volume and the heart rate, heart rate and pulmonary ventilation were measured up to submaximal level using treadmill. Heart rate and pulmonary ventilation were measured by using a microcomputer-based respiratory analyzer (Aerobic Processor: NEC-Sanei, Japan).

The subjects were 34 healthy male adults, aged 17 to 62 years. Exercises on the treadmill were gradually increased under controlled conditions to achieve stability at each heart rate level, such as +20%HR, +40%HR, +60%HR and so on. Figure 2 shows a typical pattern of heart rate change and ventilation volume during graded exercise test using treadmill and these findings indicate the correlation between the two values. Figure 3 shows the difference of heart rate-ventilation volume relationships among the subjects.

According to these findings, heart rate at resting condition (base HR), difference between heart rate in each graded exercise and base HR (ΔHR), ΔHR/base HR, age, height, weight, BMI (body mass index) were selected as initial explanatory variables for multiple regression equation to predict the ventilation volume.

Statistical processing in preparing to predict pulmonary ventilation from heart rate was performed using the multiple regression analysis program in SAS.

RESULTS AND DISCUSSION

Figure 4 shows the resultant regression equation for predicting the ventilation volume from heart rate. Base HR, ΔHR, height, weight and age remained as significant explanatory variables. Differences between the predicted pulmonary ventilation volume obtained by this equation and observed pulmonary ventilation are shown in Figure 5. The percentage of error at each heart rate level was less than 20%, for 25

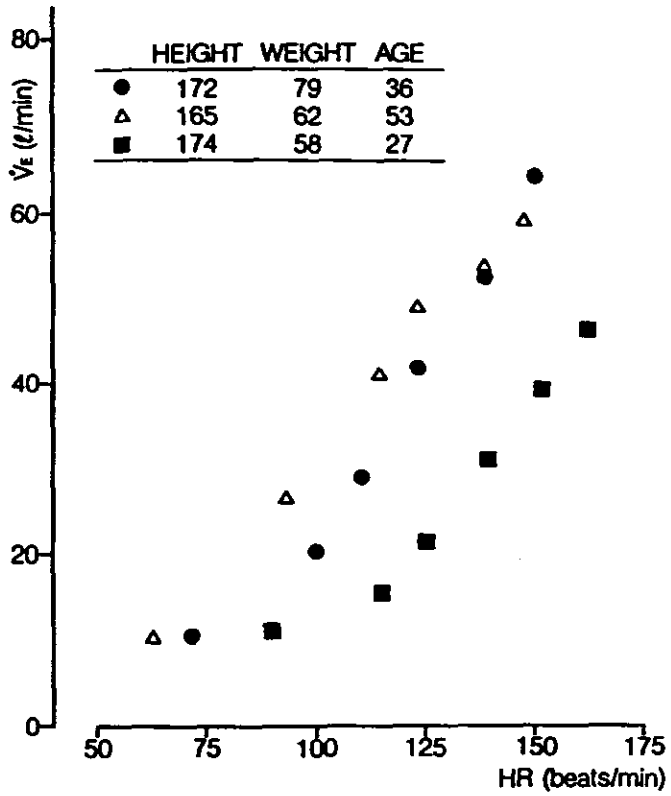

Figure 3. Difference of HR-$\dot{V}_E$ relationships among subjects.

subjects, the differences were less than 10% in each exercise level.

Figure 6 shows a sample of graphic of 1 hour monitoring. The upper photograph abbreviations mean the following, VE: ventilation volume predicted from heart rate (liter/min), BT, ET: body and ambient temperature (centidegree), DC: dust concentration (mg/cubic m), MI: indices of movement. In the lower photograph, Intake means the predicted exposure (mg) that dust concentration was multiplied by predicted ventilation volume.

To assess personal exposure better, measurement of ventilation volume is indispensable.[5] There are some methods for measuring ventilation volume as following. The first method is direct measurement of the exhalation or inhalation volume and there are several techniques for performing this. However, the subject must wear a mask or mouthpiece. This is uncomfortable, therefore the subject is under an additional amount of determined physical stress, including the increase of respiratory resistance due to wearing the equipment. Because of this, actual ventilation volume measurement may not be possible due to increase. In one indirect measurement method, ventilation volume is calculated from movement of the thorax. With this method, it is easy to see the strong correlation between movement of the chest and the ventilation volume in a state of physical rest.[6] However, accurate measurement during physical exertion is difficult.

Kucharski confirmed high correlation between heart rate and ventilation volume, and developed a personal dust sampler in which sampling air flow rate varies depending on heart rate. This sampler has been the sole device available for measuring

$$\text{Log } \dot{V}_E = 0.00938 \times X_1 + 0.00422 \times X_2 + 0.00119 \times X_3 + 0.00222 \times X_4 + 0.00335 \times X_5 - 0.0439$$

X_1: ΔHR
X_2: HEIGHT
X_3: WEIGHT
X_4: AGE
X_5: base HR

Figure 4. Regression equation calculated from the data of 34 healthy male volunteers.

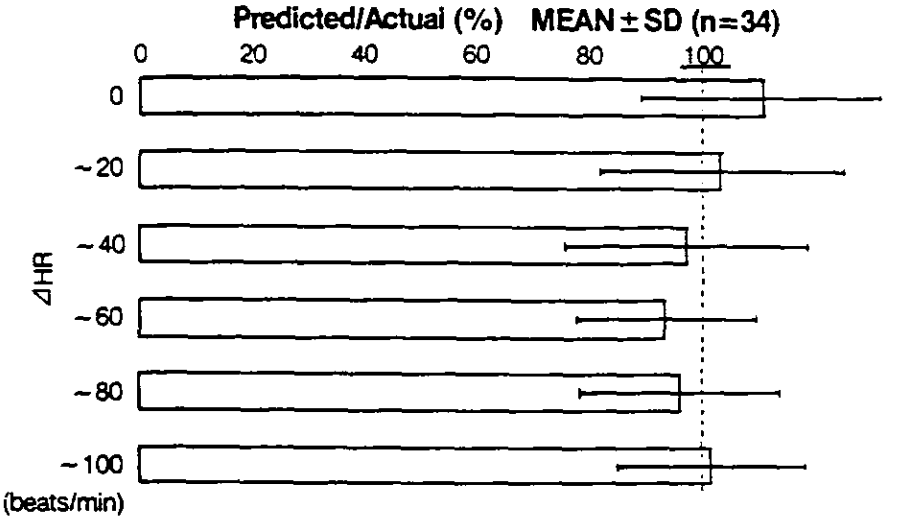

Figure 5. Difference between predicted values and actual values at each heart rate level.

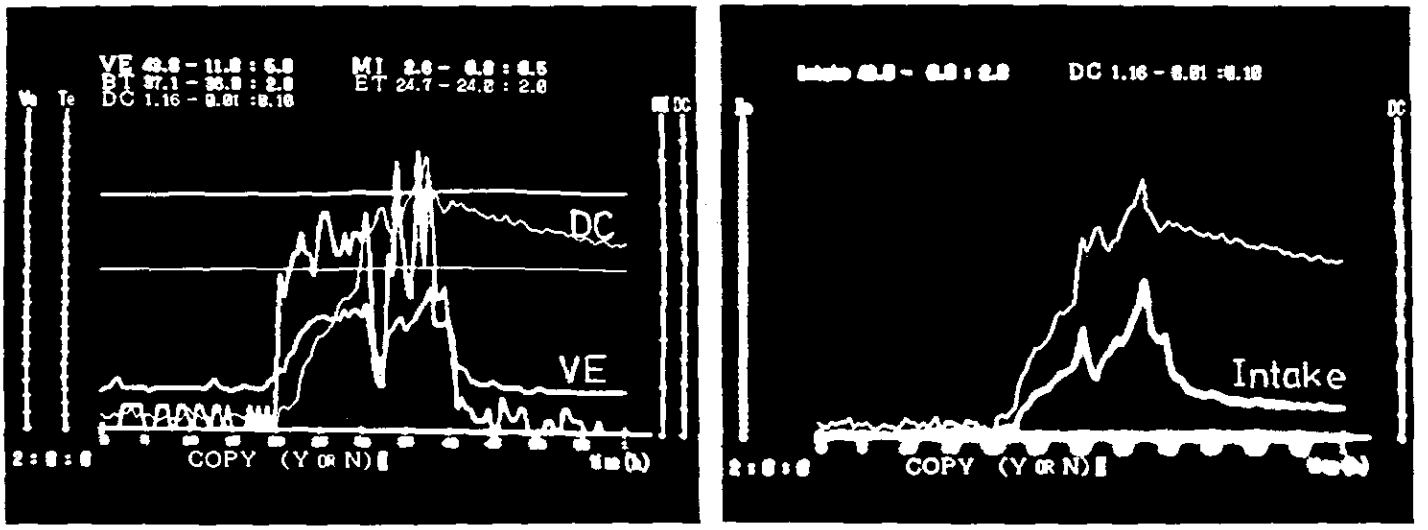

Figure 6. A sample of graphic output on VDU.

exposure in association with pulmonary ventilation.[7] We also observed the high correlation between the heart rate and the ventilation volume and made a prediction equation. Advantages of our system compared with that of Kucharski are to evaluate the real time dust concentration and ventilation which are useful for assessing the various work conditions.

At actual workplaces, exercise is varied, and there are various factors affecting pulmonary ventilation and heart rate, such as breath-holding and mental stress. However, differences in values due to differences in type of exercise were permissible in view of purpose of our system.[4]

The problems, such as deposition rate of particles depending on their size distribution which is an important factor for assessing actual exposure, and development of more unrestrictive methods to measure heart rate, still remain unsolved.

CONCLUSION

1. We developed a system that continuously measures airborne dust concentration and heart rate to predict ventilation volume, simultaneously.
2. Ventilation volume can be calculated with the heart rate. The difference between the predicted value and the actual recorded value is negligible for practical use.
3. With this instrument, the actual intake volume could be more accurately evaluated compared with the methods heretofore.
4. Electrodes of heart rate sensor is slightly restrictive for workers. Improvement is necessary in this point.

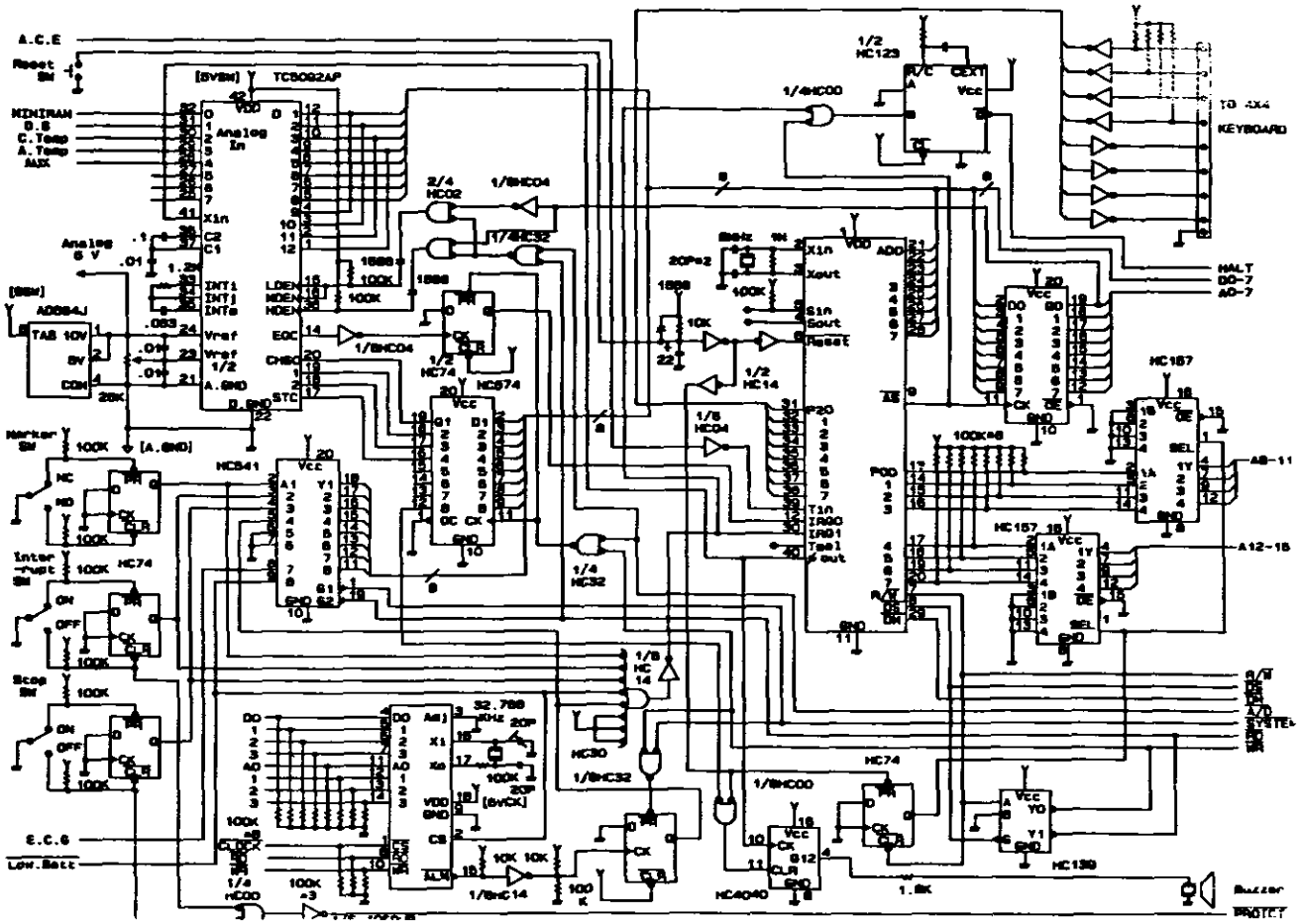

REFERENCES

1. Bjorn, E., Astrand, P.O., et al: Effect of training on circulatory response to exercise. *J. Appl. Physiol.* 24:518-528 (1968).
2. Consolazio, C.F., Nelson, R.A., et al: Body weight, heart rate, and ventilatory volume relationships to oxygen uptakes. *Am. J. Clin. Nutrition* 24:1180-1185 (1971).
3. McMahon, T.A., Brain, J.D., Lemott, S.: *Species differences in aerosol deposition, inhaled particles IV*, part 1, pp. 23-45, Pergamon Press, Oxford (1977).
4. Satoh, T., Higashi, T., Sakurai, H.: Development of a new device for personal exposure measurement considering ventilation volume. *XXII International Congress on Occupational Health*, Sydney, Australia (27 September–2 October, 1987).
5. Sharky, B.J.: Pulse rate and pulmonary ventilation as predictors of human energy cost. *Ergonomics* 9:223-227 (1966).
6. Hill, S.L., Blackburn, J.P., Williams, T.R.: Measurement of respiratory flow by inductance pneumography. *Medical & Biological Engineering & Computing*. 20:517-518 (1982).
7. Kucharski, R.: A personal dust sampler simulating variable human lung function. *Brit. J. Industr. Med.* 37:194-196 (1980).

ACKNOWLEDGEMENT: I wish to express my thanks to Mr. Kouki Isago (RICOH Co.) for his valuable assistance in the design of the DEM-1 and Mr. Yuji Noritake (Ricoh Techno-Research Co.) for his contribution to complete the data processing soft-ware.